

Kinetic Parameter Estimation from SPECT Cone-Beam Projection Measurements *

Ronald H. Huesman[†], Bryan W. Reutter[†], G. Larry Zeng[‡] and Grant T. Gullberg[‡]

[†] Center for Functional Imaging, Lawrence Berkeley National Laboratory,
University of California, Berkeley, CA 94720, USA

[‡] Department of Radiology, University of Utah, Salt Lake City, UT 84132, USA

Introduction

Kinetic parameters are commonly estimated from dynamically acquired nuclear medicine data by first reconstructing a dynamic sequence of images and subsequently fitting the parameters to time activity curves generated from regions of interest overlaid upon the reconstructed image sequence. Since SPECT data acquisition involves movement of the detectors (fig 1) and the distribution of radiopharmaceutical (fig 2) changes during the acquisition the image reconstruction step can produce erroneous results that lead to biases in the estimated kinetic parameters. If the SPECT data are acquired using cone-beam collimators wherein the gantry rotates so that the focal point of the collimators always remains in a plane, the additional problem of reconstructing dynamic images from insufficient projection samples arises. The reconstructed intensities will also have errors due to insufficient acquisition of cone-beam projection data, thus producing additional biases in the estimated kinetic parameters.

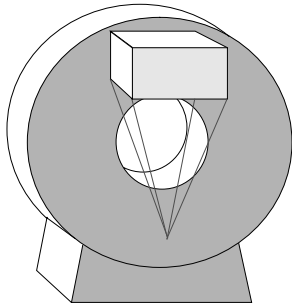


Figure 1: Cone-beam SPECT scanner.

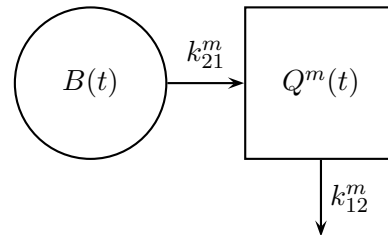


Figure 2: Compartmental model for ^{99m}Tc-teboroxime in the myocardium.

To overcome these problems we have investigated the estimation of the kinetic parameters directly from the projection data by modeling the data acquisition process of a time-varying distribution of radiopharmaceutical detected by a rotating SPECT system with cone-beam collimation. To accomplish this it was necessary to parameterize the spatial and temporal distribution of the radiopharmaceutical within the SPECT cone-beam field of view. We hypothesize that by estimating directly from cone-beam projections instead of from reconstructed time-activity curves, the parameters which describe the time-varying distribution of radiopharmaceutical can be estimated without bias.

*This work was supported by U.S. Department of Health and Human Services grant R01-HL50663 and by U.S. Department of Energy contract DE-AC03-76SF00098.

The direct estimation of kinetic parameters from the projection measurements has become an active area of research. However, to our knowledge no one has accomplished direct estimation from full 3D projection data sets. In the work at the University of Michigan, Chiao et al. [1, 2] performed estimates of ROI kinetic parameters for a one-compartment model and estimates of parameters of the boundary for the ROIs from simulated transaxial PET measurements. They demonstrated that the biases in the kinetic parameter estimators were reduced by allowing for estimators of the boundary of the ROIs to be included in the estimation process. In other work at the University of British Columbia, Limber et al. [3] fit the parameters of a single exponential decay (to model fatty acid metabolism in the heart) directly from simulated projections acquired with a single rotating SPECT detector system.

Estimation of time-activity curves from projections has been investigated by several groups. We have described a method to estimate the average activity in a 2D region of interest [4], and Defrise et al. [5] extended these ideas to 3D. To compensate for physical factors such as attenuation and detector resolution, Carson [6] described a method to estimate activity density assumed to be uniform in a set of regions of interest using maximum likelihood, and Formiconi [7] similarly used least squares.

The present research builds on the work of Carson and Formiconi as well as on our previous research [8] wherein a one-compartment model fit dynamic sequences in a 3×3 array directly from projection measurements. This work showed a bias in estimates from the reconstructed time activity curves, which were eliminated in estimating the parameters directly from the projections. The estimation was performed in a two step process: by first estimating the exponential factors using linear time-invariant system theory, then estimating the multiplicative factors using a linear estimation technique.

The research presented here formulates the problem as a minimization of one non-linear estimation problem for a 3D time-varying distribution measured with planar orbit cone-beam tomography. A one-compartment model is assumed for the simulated myocardium tissue with a known blood input function, which would correspond to the kinetics of teboroxime in the heart [9, 10]. Parameters are estimated by minimizing a weighted sum of square differences between the projection data and the model predicted values for a rotating detector SPECT system with cone-beam collimators. The estimation of parameters directly from projections is compared with estimation of kinetic parameters from tomographic determination of time-activity curves for four regions of interest.

Estimation of Kinetic Parameters Directly from Projections

The parameters are determined from a model of the projection data that assumes a one-compartment kinetic model for each tissue type as shown in fig 2. The expression for uptake in tissue type m , is:

$$Q^m(t) = k_{21}^m \int_0^t B(\tau) e^{-k_{12}^m(t-\tau)} d\tau = k_{21}^m V^m(t) , \quad (1)$$

where $B(t)$ is the known blood input function, k_{21}^m is the uptake parameter, and k_{12}^m is the washout parameter. Total activity in the tissue is given by:

$$Q^m(t) + f_v^m B(t) = k_{21}^m V^m(t) + f_v^m B(t) , \quad (2)$$

where f_v^m is the fraction of vasculature in the tissue.

This analysis starts with an image segmented into blood pool, M tissue types of interest, and background as is schematically shown in fig 3. In order to obtain tissue boundaries, the object (patient) is assumed motionless during data acquisition, and a reconstructed image (for example, via the projections at the time of strongest signal, or via the summed projections) is segmented to provide anatomical structure. The image intensity at each segmented region is not used. From the segmented image the lengths of the blood pool, tissue, and background regions along each projection ray for each projection angle are calculated. The number of projection rays per projection angle is denoted by N ,

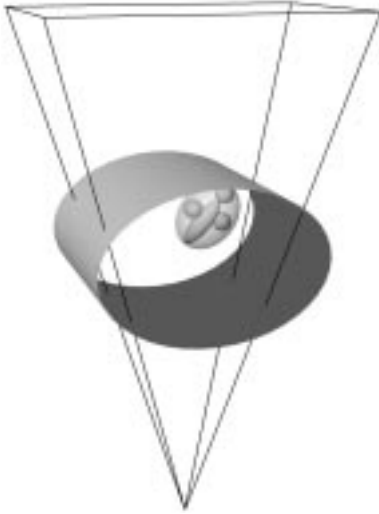


Figure 3: Phantom: The outer surface is the limit of the background activity, and the ellipsoid enclosing the small ellipsoid and three spheres represents the outer surface of the left ventricle.

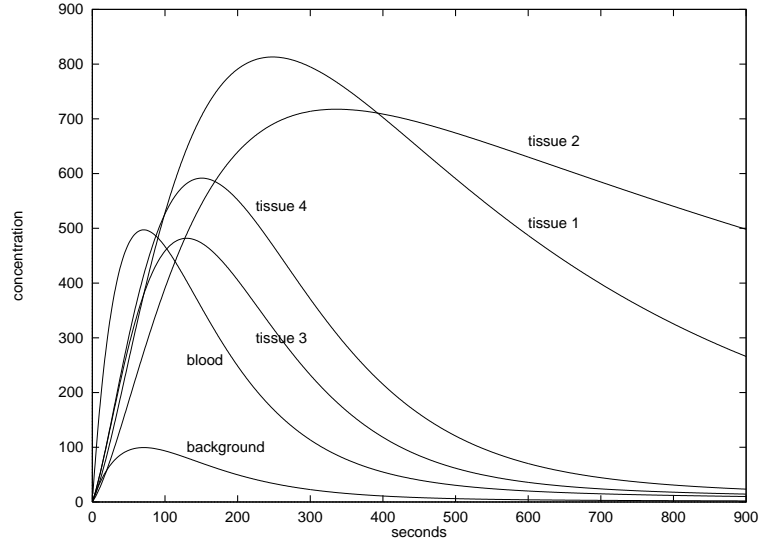


Figure 4: Time-activity curves for blood, background, and four tissue regions of interest: The bulk of the left ventricular myocardium is denoted by Tissue 2, and the spherical defects are denoted by Tissue 1, 3, 4. The Blood time-activity curve corresponds to the small ellipsoid indicating the inner wall of the left ventricle.

the number of projection angles per rotation by J , and the number of rotations by I . Thus, there are a total of IJN projection rays distributed in time and space. For a typical projection ray at angle j and position n , the length of the blood pool along the projection ray is denoted by u_{jn} , the length of the background by v_{jn} , and the length of heart tissue m by w_{jn}^m . The amplitude of the background activity is denoted by g , and the background is assumed to be proportional to the blood activity. The projection equations can be expressed as:

$$p_{ijn} = u_{jn}B(t_{ij}) + v_{jn}gB(t_{ij}) + \sum_{m=1}^M w_{jn}^m [k_{21}^m V^m(t_{ij}) + f_v^m B(t_{ij})] , \quad (3)$$

where the time t_{ij} is proportional to $j + (i - 1)J$. The constants u_{jn} , v_{jn} , and w_{jn}^m are pure geometrical weighting factors for blood, background, and tissue m , respectively, and these equations are linear in the unknowns g , k_{21}^m , and f_v^m . The nonlinear parameters, k_{12}^m , are contained in $V^m(t_{ij})$.

The criterion which is minimized by varying the model parameters is the weighted sum of squares function

$$\chi^2 = \sum_{i=1}^I \sum_{j=1}^J \sum_{n=1}^N \frac{(p_{ijn} - p_{ijn}^*)^2}{\sigma_{ijn}^2} , \quad (4)$$

where σ_{ijn} are weighting factors, and p_{ijn}^* are the measured data. Typically, σ_{ijn} is either the statistical uncertainty of the measured data or unity (for an unweighted least squares fit).

Computer Simulations

A simulation was performed to evaluate the ability to estimate the kinetic parameters directly from cone-beam projection data. A simulated image, shown in fig 3, contained background, blood, and four tissue regions of interest. The blood input function and simulated tissue activity curves are shown in fig 4. The blood input function was assumed known, and simple one-compartment models were used within four regions of interest of a simulated left ventricle of the myocardium. Boundaries of

	k_{12}^1	k_{12}^2	k_{12}^3	k_{12}^4	g	k_{21}^1	k_{21}^2	k_{21}^3	k_{21}^4	f_v^1	f_v^2	f_v^3	f_v^4
a	0.150	0.060	0.900	0.600	0.200	0.765	0.540	0.960	0.960	0.150	0.100	0.200	0.200
b	0.146	0.060	0.932	0.610	0.211	0.813	0.428	1.090	1.047	0.166	0.211	0.246	0.229
c	0.150	0.060	0.937	0.630	0.200	0.769	0.542	0.976	1.124	0.133	0.102	0.271	-0.003
d	0.150	0.060	0.900	0.600	0.200	0.765	0.540	0.960	0.960	0.150	0.100	0.200	0.200
e	0.002	0.0002	0.056	0.021	0.0001	0.010	0.001	0.082	0.043	0.017	0.002	0.038	0.029

Table 1: Results of parameter estimation: (a) simulated, (b) noiseless Feldkamp [11], (c) noiseless Formiconi [7], (d) noiseless direct, (e) direct uncertainties for 10,000,000 events. Units for k_{21} and k_{12} are min^{-1} .

the myocardial regions were assumed known, and background activity was proportional to the input function. The parameter g was the ratio of background to blood. There were 13 parameters to estimate: the amplitudes, decay rates, and vascular fractions for the four myocardial regions, and the amplitude of the overall background. The 15 minute data acquisition protocol consisted of 10 revolutions of a single-head SPECT system with cone-beam collimators, acquiring 120 angles per revolution and 48×30 lateral samples per angle. Neither attenuation nor scatter were included. Each projection had unit bin width, and line length weighting was assumed.

Parameters were estimated by minimizing a weighted sum of squared differences between the projection data and the model predicted values (eqn 4). The result of estimating the kinetic parameters directly from the projection data for the simulation is given in Table 1. Parameter estimates from conventional analysis of noiseless simulated data had significant biases (up to about 20%). Estimation of parameters directly from the noiseless projection data was unbiased as expected, because the model used for fitting was faithful to the simulation. In addition, multiple local minima were not encountered, regardless of noise levels simulated. Parameter uncertainties for 10,000,000 detected events ranged from 0.3% to 6% for wash-out parameters and from 0.2% to 9% for uptake parameters.

Summary

The combination of gantry motion and the time-varying nature of the radionuclide distribution being imaged results in inconsistent projection data sets. Estimating kinetic parameters from time-activity curves taken from reconstructed images [11] results in biases. Some of these biases are reduced and some are increased if the time-activity curves are estimated from the projection data [7]. Estimating the kinetic parameters directly from cone-beam projections removes all bias for noiseless data as expected.

References

- [1] Chiao PC, WL Rogers, NH Clinthorne, JA Fessler, and AO Hero. Model-based estimation for dynamic cardiac studies using ECT. *IEEE Trans Med Imag*, **13**(2):217–226, 1994.
- [2] Chiao PC, WL Rogers, JA Fessler, NH Clinthorne, and AO Hero. Model-based estimation with boundary side information or boundary regularization. *IEEE Trans Med Imag*, **13**(2):227–234, 1994.
- [3] Limber MA, MN Limber, A Celler, JS Barney, and JM Borwein. Direct reconstruction of functional parameters for dynamic SPECT. *IEEE Trans Nucl Sci*, **42**(4):1249–1256, 1995.
- [4] Huesman RH. A new fast algorithm for the evaluation of regions of interest and statistical uncertainty in computed tomography. *Phys Med Biol*, **29**(5):543–552, 1984.
- [5] Defrise M, D Townsend, and A Geissbuhler. Implementation of three-dimensional image reconstruction for multi-ring positron tomographs. *Phys Med Biol*, **35**(10):1361–1372, 1990.

- [6] Carson RE. A maximum likelihood method for region-of-interest evaluation in emission tomography. *J Comput Assist Tomogr*, **10**(4):654–663, 1986.
- [7] Formiconi AR. Least squares algorithm for region-of-interest evaluation in emission tomography. *IEEE Trans Med Imag*, **12**(1):90–100, 1993.
- [8] Zeng GL, GT Gullberg, and RH Huesman. Using linear time-invariant system theory to estimate kinetic parameters directly from projection measurements. *IEEE Trans Nucl Sci*, **NS-42**(6):2339–2346, 1995.
- [9] Smith AM, GT Gullberg, PE Christian, and FL Datz. Kinetic modeling of teboroxime using dynamic SPECT imaging of a canine model. *J Nucl Med*, **35**(3):984–995, 1994.
- [10] Smith AM, GT Gullberg, and PE Christian. Experimental verification of ^{99m}Tc -teboroxime kinetic parameters in the myocardium using dynamic SPECT: Reproducibility, correlations to flow, and susceptibility to extravascular contamination. *J Nucl Cardiol*, **3**:130–142, 1996.
- [11] Feldkamp LA, LC Davis, and JW Kress. Practical cone-beam algorithm. *J Opt Soc Am A*, **1**(6):612–619, 1984.

Disclaimer

This document was prepared as an account of work sponsored by the United States Government. While this document is believed to contain correct information, neither the United States Government nor any agency thereof, nor The Regents of the University of California, nor any of their employees, makes any warranty, express or implied, or assumes any legal responsibility for the accuracy, completeness, or usefulness of any information, apparatus, product, or process disclosed, or represents that its use would not infringe privately owned rights. Reference herein to any specific commercial product, process, or service by its trade name, trademark, manufacturer, or otherwise, does not necessarily constitute or imply its endorsement, recommendation, or favoring by the United States Government or any agency thereof, or The Regents of the University of California. The views and opinions of authors expressed herein do not necessarily state or reflect those of the United States Government or any agency thereof, or The Regents of the University of California.

Ernest Orlando Lawrence Berkeley National Laboratory is an equal opportunity employer.